lnc-Rps4l-encoded peptide RPS4XL regulates RPS6 phosphorylation and inhibits the proliferation of PASMCs caused by hypoxia

Yiying Li,[1] Junting Zhang,[1] Hanliang Sun,[1] Yujie Chen,[1] Wendi Li,[2] Xiufeng Yu,[3] Xijuan Zhao,[3] Lixin Zhang,[3] Jianfeng Yang,[4] Wei Xin,[1] Yuan Jiang,[1] Guilin Wang,[5] Wenbin Shi,[5] and Daling Zhu[1,3]

[1]Biopharmaceutical Key Laboratory of Heilongjiang Province, College of Pharmacy, Harbin Medical University, Harbin, Heilongjiang Province 150081, P.R. China; [2]College of Pharmacy, Harbin University of Commerce, Harbin, Heilongjiang Province 150081, P.R. China; [3]Central Laboratory of Harbin Medical University (Daqing), Daqing 163319, P.R. China; [4]College of Pharmacy, Harbin Medical University, Daqing 163319, P.R. China; [5]College of Medical Laboratory Science and Technology, Harbin Medical University, Daqing, Heilongjiang Province 163319, P.R. China

Pulmonary artery smooth muscle cells (PASMCs) proliferation caused by hypoxia is an important pathological process of pulmonary hypertension (PH). Prevention of PASMCs proliferation can effectively reduce PH mortality. Long non-coding RNAs (lncRNAs) are involved in the proliferation process. Recent evidence has demonstrated that functional peptides encoded by lncRNAs play important roles in cell pathophysiological process. Our previous study has demonstrated that lnc-Rps4l with high coding ability mediates the PASMCs proliferation under hypoxic conditions. We hypothesize in this study that a lnc-Rps4l-encoded peptide is involved in hypoxic-induced PASMCs proliferation. The presence of peptide 40S ribosomal protein S4 X isoform-like (RPS4XL) encoded by lnc-Rps4l in PASMCs under hypoxic conditions was confirmed by bioinformatics, immunofluorescence, and immunohistochemistry. Inhibition of proliferation by the peptide RPS4XL was demonstrated in hypoxic PASMCs by MTT, bromodeoxyuridine (BrdU) incorporation, and immunofluorescence assays. By using the bioinformatics, coimmunoprecipitation (coIP), and mass spectrometry, RPS6 was identified to interact with RPS4XL. Furthermore, lnc-Rps4l-encoded peptide RPS4XL inhibited the RPS6 process via binding to RPS6 and inhibiting RPS6 phosphorylation at p-RPS6 (Ser240+Ser244) phosphorylation site. These results systematically elucidate the role and regulatory network of Rps4l-encoded peptide RPS4XL in PASMCs proliferation. These discoveries provide potential targets for early diagnosis and a leading compound for treatment of hypoxic PH.

INTRODUCTION

Pulmonary hypertension (PH) is a pulmonary vascular disease characterized by a gradual increase in pulmonary vascular resistances, which cause symptoms of exertional dyspnea that gradually worsen toward right ventricular failure.[1–6] The pathological process of PH is complicated, involving hypoxic pulmonary vasoconstriction (HPV), pulmonary vessel remodeling (PVR), and pulmonary vascular adventitial fibrosis. PVR is the primary cause of PH and is characterized by an accumulation of different vascular cells (pulmonary artery smooth muscle cells [PASMCs], endothelial cells, fibroblasts, myofibroblasts, and pericytes) in the pulmonary arterial wall, a loss of pre-capillary arteries, and an exaggerated perivascular infiltration of inflammatory cells.[6] The excessive proliferation of PASMCs caused by hypoxia is an important cause of vascular regeneration.[7,8] Finding effective ways to inhibit the proliferation of PASMCs caused by hypoxia is beneficial to the early treatment of PH.

Long non-coding RNAs (lncRNAs) as a research hotspot in recent years have been found to play functions *in vivo*.[9–11] It has been reported that lncRNAs can exert regulatory functions through multiple channels: as a sponge for adsorbing microRNA (miRNA),[12,13] as a support structure to binding protein,[14] as a bridge to close the two chromatin regions to activate transcription of a chromatin region,[15] and many more. It also has been found that some lncRNAs can inhibit the proliferation of PASMCs caused by hypoxia.[16–20] However, the lncRNAs involved in the process and the regulating mechanisms still need to be explored.

Contrary to traditional knowledge that lncRNAs were considered to have non-coding ability, recent studies have proved that some lncRNAs have one or more short open reading frames (sORFs) and peptide/protein-coding potential. Studies have shown that lncRNAs with sORFs mediate many biological activities by the peptides they encode.[21,22] It is possible that lncRNAs encoding peptides serve as functional key nodes for new therapeutic targets or potential leading compounds in many diseases. Therefore, these peptides should be investigated as a new therapeutic strategy for PH.[23]

A

B

ID	Label	Coding probability	Peptide length(aa)	Fickett score	Isoelectric point	ORF integrity
NR_003634.2	coding	0.998853	263	0.39987	10.2844848633	complete

C

D

E

F
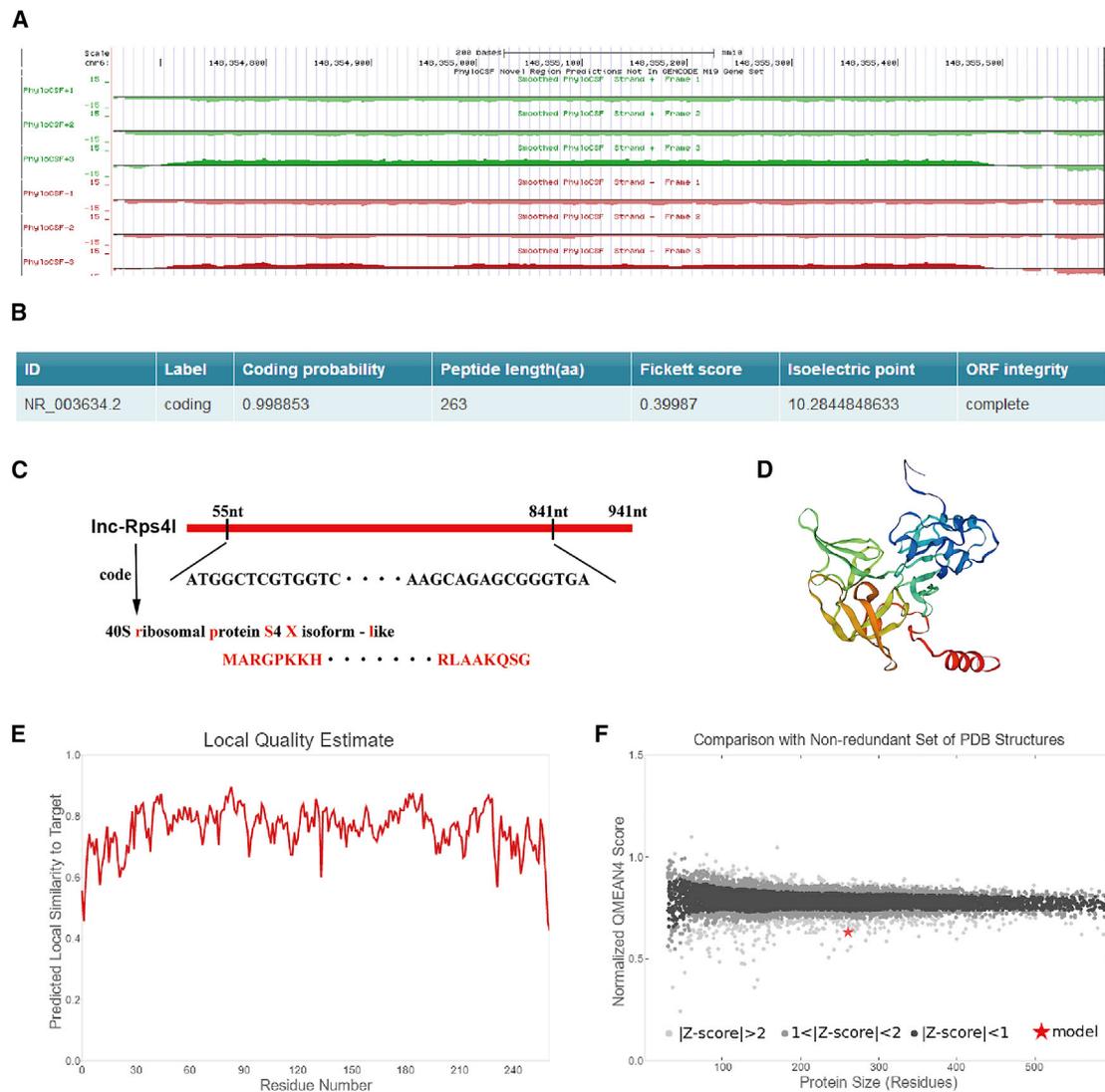
Figure 1. Rps4l encoding possibility prediction

(A) Bioinformatics prediction of the coding ability of Rps4l by PhyloCSF. (B) Bioinformatics prediction of the coding ability of Rps4l by CPC2. (C) The sequence and name of the Rps4l-encoded peptide. (D) Schematic structural model of Rps4l-encoded peptide. (E and F) Local quality estimate (E) and normalized QMEAN4 score (F) of a model of Rps4l-encoded peptide by SWISS-MODEL.

In our previous study, we found that 40S ribosomal protein S41 (Rps4l), a lncRNA that was downregulated under hypoxic conditions (Rps4l; NCBI accession number NR_003634.2), can regulate the proliferation of PASMCs through binding to interleukin enhancer-binding factor 3 (ILF3).[24] Here, we identify a new peptide encoded by Rps4l, named 40S ribosomal protein S4 X isoform-like (RPS4XL), and investigate its role in hypoxia-induced PASMCs proliferation. Compared with previous work, we have newly discovered the coding ability of Rps4l and confirmed that its encoded peptide RPS4XL can inhibit hypoxia-induced PASMCs proliferation. This encoding confirms that Rps4l plays an important function in PH both through its own binding to proteins and its regulation of PASMCs proliferation by encoding peptides.

RESULTS

Rps4l has high coding ability

Our previous research found that Rps4l is downregulated in hypoxic PASMCs and can inhibit the proliferation of PASMCs caused by hypoxia by binding to ILF3.[24] Recent studies have suggested that a lncRNA can function not only through itself, but also through its encoded peptide.[25,26] Here, we used bioinformatics websites to predict whether Rps4l regulates cell proliferation by its encoding peptides. Although Rps4l is labeled as a non-coding RNA in the NCBI gene library, we detected the presence of a region of Rps4l that might encode a peptide using PhyloCSF (Figure 1A). We further used another prediction website to test the results and reached the same result that Rps4l may encode a peptide. Fickett scores and isoelectric point

results reinforce the possibility that Rps4l has the potential ability to encode peptides (Figure 1B). We then predicted the ORF that Rps4l might encode for the peptide (Figure 1C; Figure S1). After obtaining the amino acid (aa) sequence encoding the peptide, SWISS-MODEL was used for modeling (Figures 1D–1F).

Rps4l encodes a peptide

After obtaining the extremely high coding probability of Rps4l, we tried to confirm whether this coding peptide actually exists. To confirm that Rps4l encodes a peptide, we constructed several overexpression plasmids containing the putative ORF: ORF-FLAG, ORFmut-FLAG (containing an insertion of several guanylic acid nucleotides to disrupt the ORF), and ATTORF-FLAG (in which the start codon ATG was mutated to ATT; Figure 2A). The transfection efficiency of the plasmid in mouse PASMCs is shown in Figure S2A. Subsequently, we detected the expression of FLAG by western blotting and immunofluorescence. The expression of FLAG was detected only in cells transfected with the first plasmid and was not detected in the ORF mutant or ATT mutant group. We transfected the above plasmids into PASMCs and confirmed that Rps4l encodes a peptide, as well as confirmed the initial codon (Figures 2B and 2C). In order to confirm the aa sequence of the peptide, we transfected the ORF-FLAG plasmid into PASMCs, used an anti-FLAG antibody for coimmunoprecipitation (coIP), and cut out the area of the gel corresponding to the predicted molecular weight of the peptide for use in mass spectrometry (Figure 2D). Several specific peptide segments of the Rps4l-encoded peptide RPS4XL were detected (Figure 2E; Figures S3A–S3D).

Hypoxia can cause downregulation of Rps4l-encoded peptide in PASMCs

Based on the ORF sequence of the Rps4l-encoding peptide, we named it RPS4XL. According to the aa sequence, we purified the peptide RPS4XL *in vitro*. The specificity of the antibody was detected by overexpression and interference of Rps4l (Figures S4A and S4B). The interference efficiency has been verified in a previous study.[24] We further used the antibody to assess the expression of RPS4XL *in vitro* and *in vivo*. In cultured mouse PASMCs, overexpression of Rps4l reverses the downregulation of RPS4XL caused by hypoxia. This also confirms the possibility that RPS4XL is encoded by Rps4l (Figure 3A). To determine the expression of Rps4l-encoded peptide in PH *in vivo*, we used a transgenic mice model characterized by the overexpression of Rps4l (Rps4lTg). The expression of Rps4l in different organs of overexpression transgenic mice is shown in Figures S5A and S5B. We found that hypoxia for 21 days caused downregulation of RPS4XL expression in the lungs of mice, and this phenomenon was reversed in the overexpressing Rps4l transgenic mice (Figures 3B–3D).

Rps4l regulates PASMC proliferation through its encoded peptide, RPS4XL

After finding that Rps4l encodes a peptide, RPS4XL, we examined RPS4XL's effect on the proliferation of PASMCs and found that Rps4l indeed inhibits the proliferation of PASMCs via its encoded peptide (Figures 4A–4D). MTT (3-(4,5)-dimethylthiahiazo(-z-y1)-3,5-di-phenytetrazoliumromide), bromodeoxyuridine (BrdU) incor-

poration, and immunofluorescence assays revealed that overexpression of Rps4l reversed hypoxia-induced increases in PASMC viability and proliferation, but this reversal was eliminated by mutation of Rps4l. We further examined the effect of RPS4XL on the cell cycle. Through the detection of expression of cyclin by western blot, we found that overexpression of Rps4l can inhibit the acceleration of the cell-cycle process caused by hypoxia, but this process was reversed by mutation of Rps4l (Figure 4E). Through scratch-wound assays, we assessed the migration ability of PASMCs under hypoxic conditions. Similarly, the results showed that overexpression of Rps4l could inhibit the migration of PASMCs induced by hypoxia, but this phenomenon was reversed by mutation of Rps4l (Figure 4F). Next, we detected the expression of apoptosis-related proteins caspase-3 and caspase-9 by western blot. The results showed that both Rps4l and RPS4XL does not regulate hypoxia-induced inhibition of apoptosis in PASMCs (Figures S6A and S6B). The above results prove that Rps4l can inhibit the proliferation of PASMCs by inhibiting cell-cycle progression and migration through its encoded peptide RPS4XL. At the same time, in order to more intuitively detect the effect of RPS4XL on the proliferation, we added exogenously synthesized peptides RPS4XL to PASMCs. MTT assay results show that RPS4XL does not inhibit the cell viability of basic cells (Figure 5A). But it inhibited the cell viability of PASMCs under hypoxic conditions (Figure 5B). Western blot assays revealed that the addition of exogenous RPS4XL inhibit the acceleration of cell-cycle progression caused by hypoxia (Figures 5C and 5D).

Rps4l-encoded peptide RPS4XL interacts with RPS6

To further understand the molecular mechanism by which the Rps4l-encoded peptide RPS4XL inhibits the proliferation of PASMCs, we identified proteins that interact with RPS4XL. First, we predicted proteins interacting with RPS4XL using the bioinformatics program STRING (Figure 6A) and performed Gene Ontology (GO) and Kyoto Encyclopedia of Genes and Genomes (KEGG) analyses (Figure 6B). Bioinformatics analysis predicted that RPS6, EHMT2, and NANOG interact with the Rps4l-encoded peptide RPS4XL; however, coIP and mass spectrometry revealed that only RPS6, and not EHMT2 or NANOG, interacts with RPS4XL (Figures 6C and 6D). Therefore, we further explored the role of RPS6 in the proliferation of PASMCs. Phosphorylation is a key factor in the function of RPS6. Studies have shown that phosphorylated RPS6 (p-RPS6) exerts cardioprotective effects through mTORC2-mediated protein kinase B (AKT) phosphorylation. We examined the expression of RPS6 and p-RPS6 (Ser240+Ser244) and found that they were upregulated under hypoxia *in vivo* and *in vitro*. However, upon overexpression of Rps4l, normal expression of RPS6 and p-RPS6 (Ser240+Ser244) was restored (Figures 6E and 6F). This further confirms the interaction between the Rps4l-encoded peptide RPS4XL and RPS6.

RPS4XL attenuates PASMC proliferation by inhibiting RPS6 phosphorylation

In order to investigate the effect of RPS6 on the proliferation of PASMCs, small interfering RNA (siRNA) targeting RPS6-specific sequences were made. Interference efficiency is demonstrated in Figures
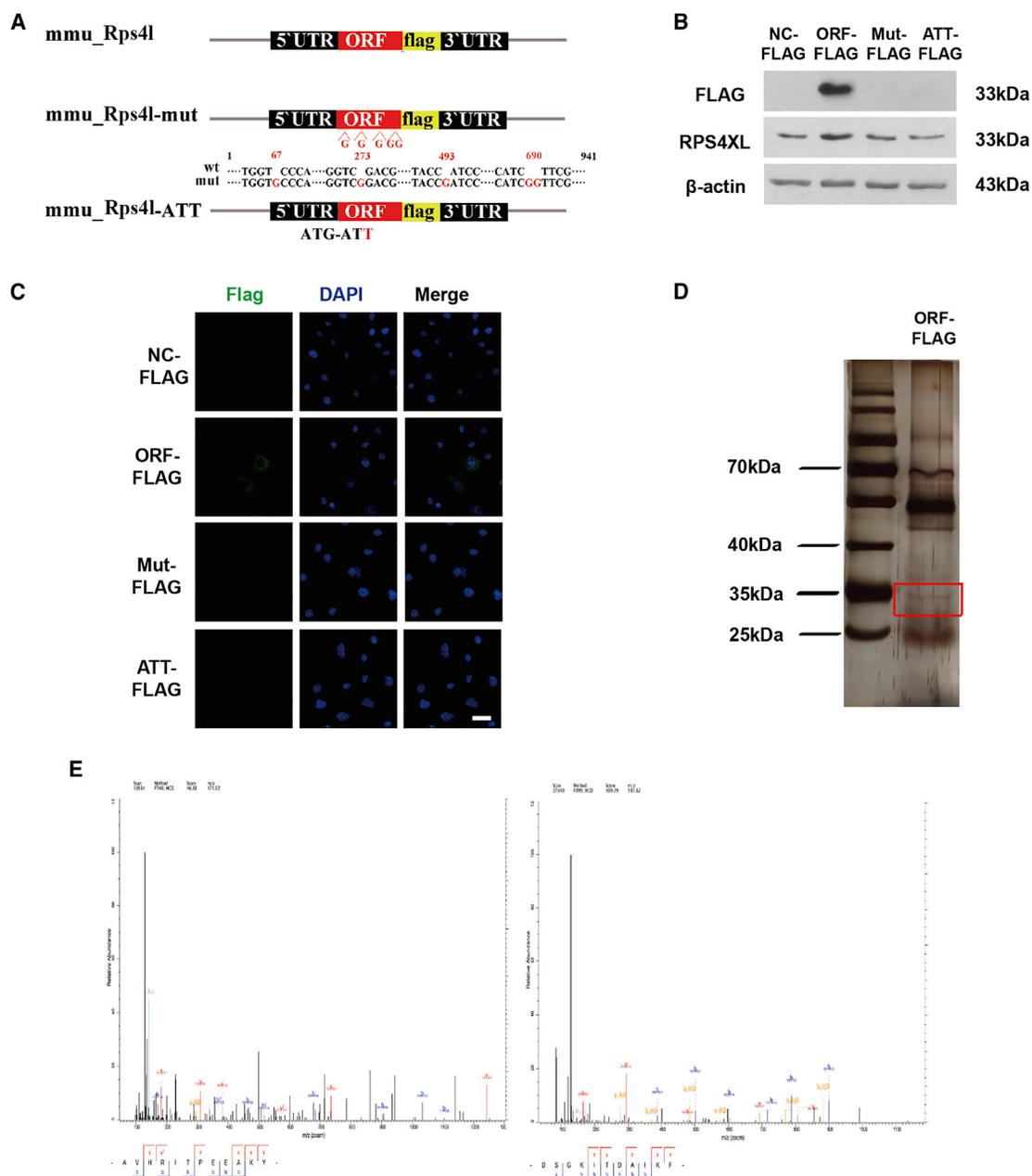
Figure 2. Rps4l encodes peptide RPS4XL

(A) Diagram of the FLAG fusion construct used for transfection. (B and C) Western blotting (WB) analysis (B) and immunofluorescence (IF) (C) of FLAG in PASMCs transfected with ORF-FLAG, ORFmut-FLAG, ATTORF-FLAG, or NC-FLAG under normoxia. (D) coIP of RPS4XL-FLAG complexes in PASMCs transfected with ORF-FLAG plasmid using anti-FLAG antibody. (E) Mass spectrometry of specific segments of Rps4l-encoded peptide RPS4XL in PASMCs. DAPI, 4',6-diamidino-2-phenylindole.

S7A and S7B. Additional MTT, BrdU incorporation, immunofluorescence, and western blotting assays showed that interference with RPS6 attenuated the hypoxia-induced increase in PASMC viability and proliferation by slowing the cell-cycle process (Figures 7A–7E). In order to further examine the regulatory relationship between RPS4XL and RPS6, we interfered with the expression of RPS6 in combination with overexpressing or mutating Rps4l. Through MTT and

western blotting assays, we found that, under hypoxic conditions, compared with overexpression of Rps4l, interfering with RPS6 after overexpression of Rps4l does not further inhibit proliferation because RPS4XL has already suppressed the expression of RPS6 and its phosphorylation. However, when the ORF of Rps4l is mutated, interference with RPS6 does exert an inhibitory effect (Figures S8A–S8C). We also added exogenous peptides in cultured RPS6 interference
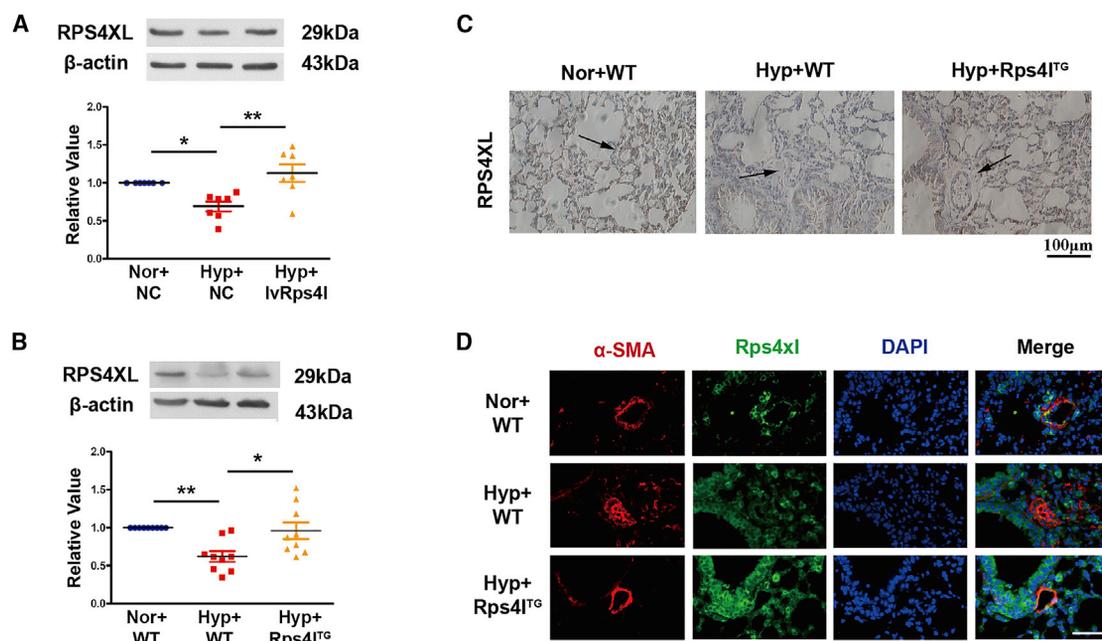
Figure 3. Confirmation of Rps4l-encoded peptide

(A) WB analysis of RPS4XL in PASMCs transfected with lvRps4l or NC under hypoxia and normoxia. (B) Lung tissues form Rps4l[Tg] and wild-type (WT) mice under hypoxia and normoxia. (C) Immunochemistry of RPS4XL in lung sections from Rps4l[Tg] and WT hypoxic and control mice (scale bar, 100 μm). (D) IF of RPS4XL in lung sections from Rps4l[Tg] and WT hypoxic and control mice (scale bar, 100 μm). All values are represented as the mean ± SEM (*p < 0.05 and **p < 0.01). Nor, normoxia; Hyp, hypoxia. NC, negative control.

PASMCs. The results showed that adding the exogenous peptides in RPS6 interference PASMCs inhibited the proliferation (Figures S8D–S8F). The above results revealed that RPS4XL can inhibit the proliferation of PASMCs caused by hypoxia by RPS6.

RPS4XL is conserved in humans and inhibits the proliferation of human PASMCs (HPASMCs) induced by hypoxia

After exploring the mechanism of RPS4XL in mice, we proceeded to verify its similar function in human PASMCs. By comparing the sequences through NCBI, we found the homologous sequences of Rps4l-encoded peptide RPS4XL in human and mouse genome (Figure S9A). And through the western blotting experiment, we found that RPS4XL expression of HPASMCs treated with hypoxia and HPASMCS of patients with PH were downregulated compared with the HPASMCs control group (Figure S9B). Information about patients with PH and how to obtain PASMCs are shown in the previous study.[27] Next, we added exogenous RPS4XL to HPASMCs to figure out whether it can also inhibit the proliferation induced by hypoxia. MTT and western blotting assays were performed, and the results show that adding exogenous peptide RPS4XL can inhibit the proliferation of HPASMCs induced by hypoxia (Figures S9C–S9E).

RPS4XL improves hypoxia-induced PH *in vivo* by regulating RPS6

After confirming that Rps4l can inhibit the proliferation of PASMCs caused by hypoxia through its encoded peptide RPS4XL binding with RPS6, we verify whether Rps4l will exert the same effect *in vivo*. We

constructed an adeno-associated virus vector 9 (AAV9) to overexpress Rps4l, mutate Rps4l, or interfere with RPS6 *in vivo*, and constructed a PH model with this vector in mice exposed to hypoxia. Overexpression efficiency and interference efficiency are demonstrated in Figures S10A and S10B.

After 21 days of hypoxia, we evaluated *in vivo* RV/(left ventricle+S), RV systolic pressure, echocardiography, and hemodynamics. We found that overexpression of lnc-Rps4l inhibits the PH induced by hypoxia, and this phenomenon was reversed by mutation of the ORF of Rps4l, suggesting that Rps4l-encoded peptide RPS4XL can regulate PH *in vivo* (Figures 8A–8E). Interfering with RPS6 *in vivo* also inhibits the PH induced by hypoxia (Figures 8F–8L). We also detected the functional link between RPS4XL and RPS6 *in vivo*. The results proved that interfering with RPS6 after overexpression of Rps4l does not further inhibit the pathological process of PH. However, after the ORF of Rps4l is mutated, interference with RPS6 exerts an inhibitory effect (Figures S11A–S11E). Taken together, these results suggested that the mechanism by which RPS4XL regulates the proliferation of PASMCs through RPS6 is also applicable *in vivo*.

DISCUSSION

In this study, we identified a novel peptide RPS4XL encoded by lnc-Rps4l, which was reduced in hypoxia-induced PH and hypoxic PASMCs. We further demonstrated that RPS4XL downregulation was associated with PASMC proliferation *in vivo* and *in vitro*, indicating that RPS4XL had a strong inhibitory effect on hypoxia-induced

A

B

C

D

E

F
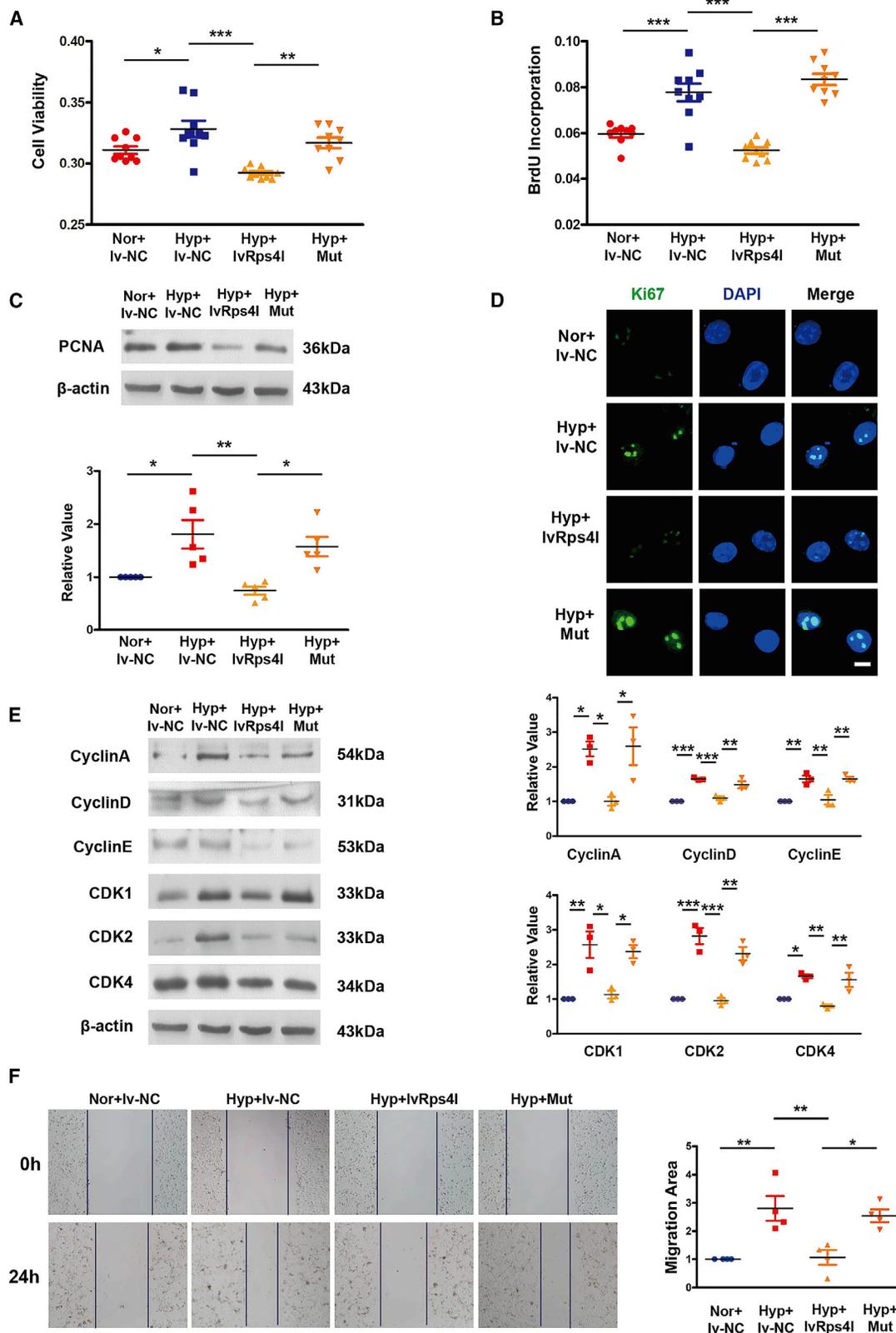
(legend on next page)

PASMCs proliferation. We also found that RPS4XL inhibits the hypoxia-induced PASMCs proliferation by binding to RPS6 following the inhibition of RPS6 phosphorylation. These results suggest that lncRNA-encoded peptide is involved in hypoxia-induced PH, which will be a key target for PASMCs proliferation.

PASMCs proliferation is a major cause of pulmonary vessel remodeling in PH. The mechanisms of PASMCs proliferation are very complex. lncRNAs are involved in the important pathological process. It had been reported that lncRNA CASC2 inhibits hypoxia-induced PASMCs proliferation and migration by regulating the miR-222/ING5 axis.[28] Under hypoxic conditions, lncRNA-MEG3 was significantly increased and isolated cytoplasmic miR-328-3p, eventually leading to expression of IGF1R, revealing a regulatory mechanism in PASMCs proliferation.[19] Our previous study showed that a novel lncRNA Rps4l was downregulated under hypoxia conditions and regulated the PASMCs proliferation through binding to ILF3.[24] In the present study, we proved that lnc-Rps4ls have an ability to encode peptide RPS4XL, which is involved in hypoxia-induced PASMCs proliferation. Our results identified that lnc-Rps4l mediates the PASMCs proliferation by Rps4l-encoded peptide RPS4XL and suggested that lncRNAs mediate cellular pathophysiological processes through very complex biological regulatory mechanisms.

Although lncRNAs are defined as non-coding RNAs, many recent studies have found that a fraction of putative small ORFs within lncRNAs are translated.[29] It has been reported that the lncRNA HOXB-AS3 encodes a conserved 53 aa peptide, and it is this peptide, not the lncRNA itself, that suppresses colon cancer growth.[22] Recent studies have shown that the LINC00961-encoded SPAR polypeptide, conserved between human and mouse, interacts with the lysosomal v-ATPase to negatively regulate mTORC1 activation and regulate muscle regeneration.[30] There are also reports that the ribosome profile can identify hundreds of lncRNAs,[31] and many lncRNAs contain sORFs.[32] lncRNAs that play a regulatory role in PH have been reported, such as Paxip1-AS1, H19, also contain sORF.[33,34] However, there are no reports of lncRNA-encoded peptides involved in hypoxia-induced PH. Here, we have confirmed that hypoxia induces the downregulation of Rps4l, which reduces the production of the Rps4l-encoded peptide RPS4XL. Our findings uncover a complex regulatory mechanism of metabolism of proliferation of PASMCs in PH via a peptide encoded by Rps4l.

The studies have shown that 28.6% to 81.0% of lncRNAs bind to ribosomes.[35] Some of lncRNAs have the ability to translate into small peptides.[36] RPS6 is one of the core proteins of ribosomal 40S subunits and influences protein synthesis by binding mRNA, tRNA, and protein

translation initiation factors.[37] Phosphorylation is a key factor that RPS6 regulates post translation.[38,39] Five highly conserved serine phosphorylation sites, including ser236, ser235, ser240, ser244, and ser247, have been identified at RPS6 C′ end.[39] Our data showed that Rps4l-encoded peptide RPS4XL interacts with RPS6 and interference with RPS6 attenuates the hypoxia-induced increase in PASMC viability and proliferation via slowing the cell-cycle process. We further proved that RPS4XL encoded by lnc-Rps4l inhibits the hypoxia-induced PASMCs proliferation by regulating RPS6 phosphorylation at Ser240 and Ser244 sites. Our study elucidates the mechanism of RPS4XL encoded by lnc-Rps4l regulating cell proliferation from the target protein of RPS6 and the RPS6 phosphorylation sites. In view of the fact that RPS6 is related to the regulation of some PH-related factors, such as HSP90, Pim-1, CHK1, etc.,[40–43] our findings indicate that RPS4XL may mediate the pathway of PH-related factors through RPS6 and ultimately affect the pathological process of hypoxia-induced PH. The discovery of the interaction between RPS4XL and RPS6 provides a basis for the in-depth study of RPS6 regulatory pathways in hypoxia-induced PH.

The addition of exogenous peptides undoubtedly further verified our conclusions. We synthetized the exogenous peptide RPS4XL and added it to PAMSCs. This provides direct evidence that RPS4XL can inhibit hypoxia-induced PASMCs proliferation. Its conservation in human PASMCs and its function have also been verified and further confirmed the important regulatory role of RPS4XL in PH. This phenomenon provides new ideas for the treatment of PH, and more research on the function of RPS4XL will be carried out in the future.

Although the lncRNA-encoded peptides we have known are shorter in length,[25,36] we do not doubt the existence of RPS4XL as a lncRNA Rps4l-encoded peptide and its regulatory value on PASMCs proliferation. Rps4l was labeled as a non-coding RNA in our previous cognition and database. Our previous study proved that Rps4l serves as a functional non-coding RNA by binding to ILF3 to regulate the expression of HIF-1α.[24] And now we have found that Rps4l has an ORF, and its coding peptide RPS4XL is exactly expressed in PASMCs and plays a crucial regulatory role. Although its ORF is long, similar to the presence of mRNA, its domain is very different from mRNA. As we all know, mRNA has longer 5′ UTR and poly(A) tails,[44,45] and these are not found on Rps4l. From this view, we speculate that Rps4l may have a different translation mechanism than mRNA. If its specific translation mechanism can be further developed, then the study of lncRNA-encoded peptides and their role in diseases will be further advanced.

A large number of studies have clearly shown that miRNA-based therapies have beneficial effects in preclinical models, but there are

Figure 4. Rps4l regulates PASMC proliferation through its encoded peptide, RPS4XL
(A) MTT assay in hypoxic and control PASMCs transfected with lvRps4l, ORFmut, or lv-NC. (B) BrdU incorporation assay in hypoxic and control PASMCs transfected with lvRps4l, ORFmut, or lv-NC. (C) WB analysis of PCNA in hypoxic and control PASMCs transfected with lvRps4l, ORFmut, or lv-NC. (D) IF of Ki67 (scale bar, 10 μm) in hypoxic and control PASMCs transfected with lvRps4l, ORFmut, or lv-NC. (E) WB analysis of cyclin A, cyclin D, cyclin E, CDK1, CDK2, and CDK4 in hypoxic and control PASMCs transfected with lvRps4l, ORFmut, or lv-NC. (F) Scratch-wound assays in hypoxic and control PASMCs transfected with lvRps4l, ORFmut, or lv-NC. All values are represented as the mean ± SEM (*p < 0.05, **p < 0.01, and ***p < 0.001; n ≥ 3).
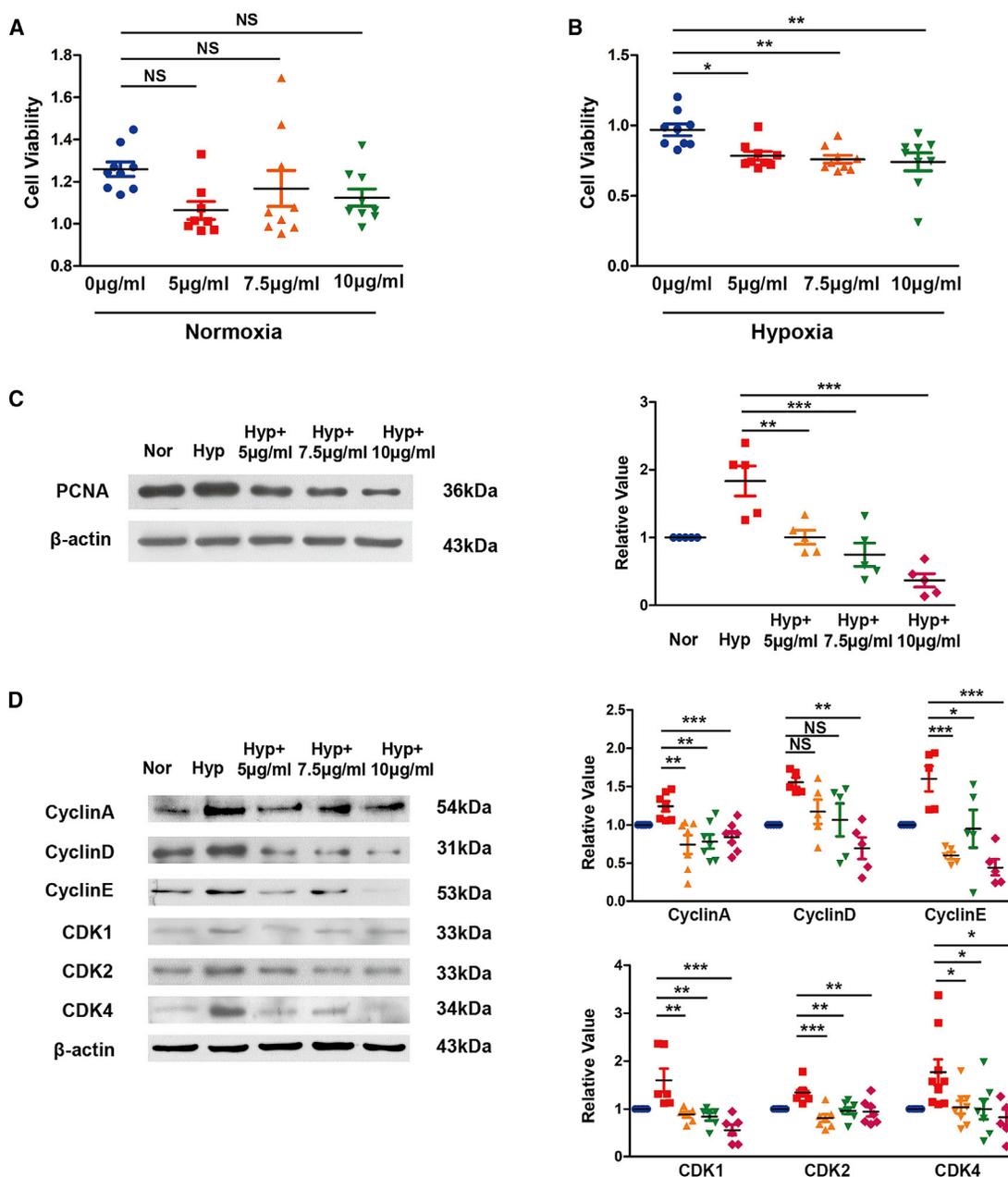
Figure 5. The peptide RPS4XL inhibits the proliferation of PASMCs induced by hypoxia

(A) MTT assay in PASMCs treated with RPS4XL with concentrations of 5 μg/mL, 7.5 μg/mL, or 10 μg/mL under normoxia. (B) MTT assay in PASMCs treated with RPS4XL with concentrations of 5 μg/mL, 7.5 μg/mL, or 10 μg/mL under hypoxia. (C and D) WB analysis of PCNA (C) and WB analysis of cyclin A, cyclin D, cyclin E, CDK1, CDK2, and CDK4 (D) in hypoxic and control PASMCs treated with RPS4XL with concentrations of 5 μg/mL, 7.5 μg/mL, or 10 μg/mL. All values are represented as the mean ± SEM (*p < 0.05, **p < 0.01, ***p < 0.001, and NS, no significance; n ≥ 3).

currently no clinical trials using lncRNA as a therapeutic target in PH.[46,47] It had been reported that lncRNAs are a key regulator of the pathogenesis of PH, suggesting that lncRNAs may serve as the potential targets for PH therapies. Our study proved that lnc-Rps4l has the ORF with the coding ability to encode peptide RPS4XL, and by binding to RPS6, the new peptide RPS4XL plays a crucial role in

regulating hypoxia-induced PASMCs proliferation. Therefore, our results provide new potential targets and lead compounds for drug development for lncRNA-dependent PH therapies.

There are some limitations in our study. The role of RPS6 phosphorylation sites regulated by RPS4XL on proliferation should be
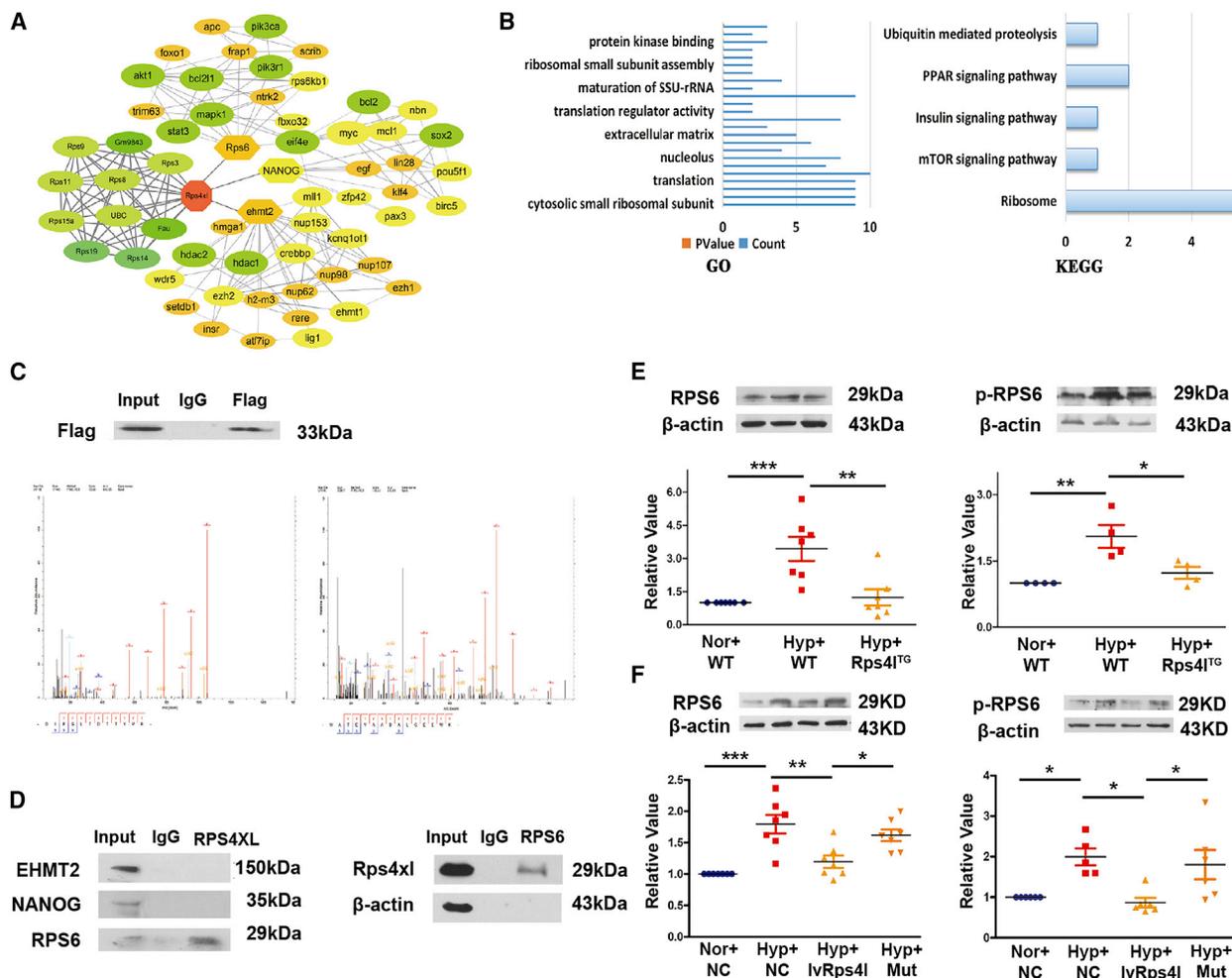
Figure 6. Rps4l-encoded peptide RPS4XL interacts with RPS6

(A) Bioinformatics prediction of network of proteins interacting with Rps4l-encoded peptide RPS4XL by STRING. (B) GO and KEGG analysis of proteins interacting with Rps4l-encoded peptide RPS4XL. (C) WB analysis of FLAG in PASMCs transfected with ORF-FLAG plasmid under normoxia after coIP using anti-FLAG antibody. Mass spectrometry of specific segments of RPS6. (D) WB analysis of EHMT2, NANOG, RPS6, and Rps4l-encoded peptide RPS4XL in PASMCs after coIP using anti-RPS4XL and anti-RPS6 antibodies under normoxia. (E and F) WB analysis of RPS6 and p-RPS6 in (E) lung tissues from Rps4l^Tg and WT mice and (F) hypoxic and control PASMCs transfected with lvRps4l, ORFmut, or NC. All values are represented as the mean ± SEM (*$p < 0.05$, **$p < 0.01$, and ***$p < 0.001$; n ≥ 3).

determined, and other phosphorylation sites of RPS6 regulated by RPS4XL and their role in PH also need to be revealed. In addition, RPS6 phosphorylation is regulated by serial protein kinases such as casein kinase 1 (ck1)-selective phosphorylation of ser247 sites.[48] The function of RPS6 phosphorylation can be carried out through PI3K/AKT/mTOR and other singling pathways.[49,50] Therefore, upstream and downstream mechanisms of RPS6 phosphorylation regulated by lnc-Rps4l-encoded peptide should exploited in PH.

In conclusion, our results indicate that the lncRNA-Rps4l-encoded peptide RPS4XL plays a significant and unique role in hypoxia-induced PASMCs proliferation. We have demonstrated that RPS4XL has a critical regulatory role in proliferation *in vivo* and *in vitro* by the interaction with RPS6, leading to RPS6 phosphorylation. This

finding suggests that lncRNA-Rps4l-encoded peptide RPS4XL may serve as a potential target and a leading compound for the treatment of PH.

MATERIALS AND METHODS
Animals

Animal care and use conformed to the Guide for the Care and Use of Laboratory Animals (National Institutes of Health Publication 85-23, revised 1996). All experimental procedures in animals were carried out and conducted in compliance with NIH guidelines and were approved by the Institutional Animal Care and Use Committee of Harbin Medical University. C57BL/6 mice were obtained from the Experimental Animal Center of Harbin Medical University, and C57BL/6 mice with blunt-CAG promoter-driven
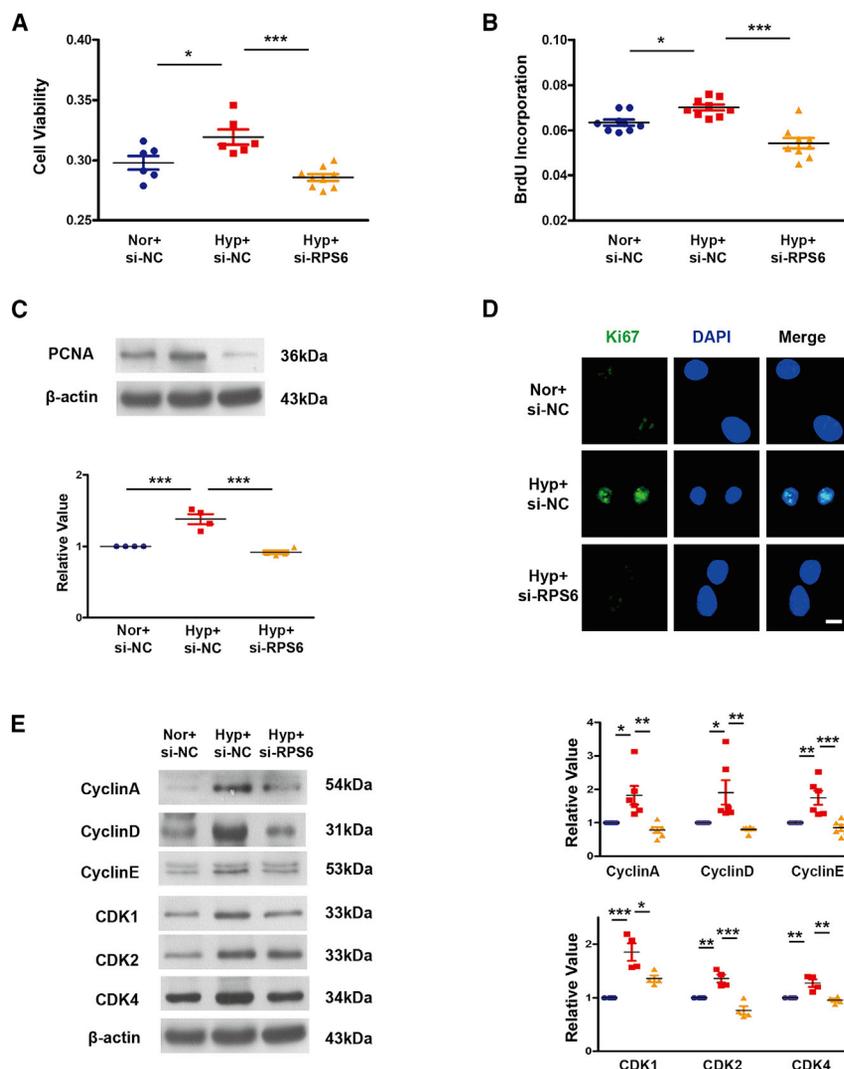
Figure 7. Interference with RPS6 can inhibit the proliferation of PASMCs caused by hypoxia

(A) MTT assay in hypoxic and control PASMCs transfected with si-RPS6 or si-NC. (B) BrdU incorporation assay in hypoxic and control PASMCs transfected with si-RPS6 or si-NC. (C) WB analysis of PCNA in hypoxic and control PASMCs transfected with si-RPS6 or si-NC. (D) IF of Ki67 (scale bar, 10 μm) in hypoxic and control PASMCs transfected with si-RPS6 or si-NC. (E) WB analysis of cyclin A, cyclin D, cyclin E, CDK1, CDK2, and CDK4 in hypoxic and control PASMCs transfected with si-RPS6 or si-NC. All values are represented as the mean ± SEM (*p < 0.05, **p < 0.01, and ***p < 0.001; n ≥ 3).

Isolation and culture of mouse PAMCs

20–30 g male C57BL6 mice with SPF grade were obtained from the Experimental Animal Center of Harbin Medical University, and the mice from both control and hypoxia groups were anesthetized with pentobarbital sodium. The pulmonary artery vessels were separated and endothelial layer scraped. The vessels were cut into small pieces, and smooth muscle cells were digested with type II collagenase (1 mg/mL). The cells were cultured with 20% fetal bovine serum (FBS) DMEM after centrifugation. The content of oxygen in normal incubator is 21% and that in hypoxia is 3%.

RNA extraction

The cells were lysed by TRIzol (Invitrogen, Carlsbad, CA, USA) according to the manufacturer's protocol after washing with PBS 3 times. After lysis with TRIzol, chloroform was added, and the cells were vortexed and centrifuged. The supernatant was removed by suction. Isopropanol was then added, the sample was centrifuged, and the precipitate was washed with 75% ethanol, air-dried, and dissolved. The optical density was measured using a microplate reader (Shimadzu Corporation, Japan). A S1000 thermal cycler with random hexamer primers (Thermo Fisher, USA) or oligo (dt) and random primers (Haigene, China) was used for reverse transcription of the total RNA obtained.

overexpression of Rps4l were obtained from Beijing Weitongda Biotech meeting criteria including SPF level, male, and 20–30 g weight. The mice were randomly divided into normal groups and hypoxic groups. The normal group was placed in a normal culture environment, with inhaled oxygen concentration at 21%, while the hypoxic group experienced inhaled oxygen concentration at 10% inside an animal hypoxia chamber. All the groups were cultured for 21 days. The chamber gas was monitored continuously using an oxygen analyzer (Model 1175; Servomex, Crowborough, UK). Excess CO₂ was removed by continuously recirculating gases from the chamber through soda lime. Excess humidity and ammonia were removed with a cooled condensing unit and an activated charcoal filter (Carbon-Cap 150; Whatman, Maidstone, UK), respectively. Pentobarbital sodium was injected intraperitoneally at a concentration of 1% and 40 mg/kg to anesthetize mice for index detection.[51,52]

Real-time PCR

The isolated RNA was reverse transcribed into cDNA using a reverse transcription kit (Takara, Dalian, China). The amplification reaction was performed for 1 min at 95°C and 15 min at 95°C, followed by 40 cycles at 95°C for 15 s and 52°C for 15 s. All qRT-PCR reactions were performed in duplicate. The primers were as follows: Rps4l forward, 5′-CATCGGCGTCATCACCAACC-3′ and reverse, 5′-TCCCTCA-GAGTCCACTTCACC-3′; RPS6 forward, 5′-GATGATGTCCGC-CAGTATGTTG-3′ and reverse, 5′-AGCCTCCTCCTTGTTCTTCT-TAG-3′.

Figure 8. RPS4XL and RPS6 regulates hypoxia-induced PH *in vivo*

(A) Right ventricular systolic pressure (RVSP). (B) RV/left ventricular (LV)+S weight ratio. (C) Pulmonary artery acceleration time (PAAT). (D and E) PAVTI (D) and H&E (E) staining (scale bar, 200 μm) of hypoxic mouse model infected with AAV9-lv-NC, AAV9-lv-Rps4l, AAV9-lv-mut, and AAV9-si-NC. (F–J) RVSP (F), RV/ (LV+S) weight ratio (G), PAAT (H), PAVTI (I), and H&E (J) staining (scale bar, 200 μm) of hypoxic mouse model infected with AAV9-si-NC, AAV9-si-RPS6, and AAV9-lv-NC. All values are represented as the mean ± SEM (*p < 0.05, **p < 0.01, and ***p < 0.001; n ≥ 3).

Silver stain

The silver staining of the western blotting gel was performed following the protocol of rapid printing kit provided by Beyotime (Shanghai, China). After the electrophoresis was over, the gel was placed in about 100 mL of fixative and then on a shaker at room temperature for 20 min. The configuration method of the fixative was to add 50 mL ethanol, 10 mL acetic acid, and 40 mL ultrapure water in sequence. Then the fixative was discarded and 100 mL of 30% ethanol was added. After shaking on a shaker for 10 min, the ethanol was discarded, 200 ultrapure water was added, and shake for another 10 min. After discarding the ultrapure water, 100 mL of silver dye sensitizer was added and shaken on a shaker for 2 min. The sensitizer was discarded, ultrapure water was added and shaken for wash twice for 2 min each time. Then the ultrapure water was discarded and 100 mL silver solution was added. After shaking for 10 min, the solution was washed again with ultrapure water for 1 min. Then the liquid was discarded, silver dye color developing solution was added, shaken for 3 min, the liquid discarded, and 100 mL silver dye stop solution added. After shaking for 10 min, the liquid was discarded and ultrapure water was added to wash.

coIP assay

Protein samples were extracted from PASMCs using procedures described previously. Cell lysates were incubated with anti-FLAG antibody for 6 h and incubated with protein A+G magnetic beads overnight. The protein complex was precipitated by centrifugation and washed 5 times with PBS. The protein was separated by heating with protein loading buffer.

Mass spectrometry

The corresponding molecular weight or protein solution was prepared and analyzed by Beijing Bio-Tech Pack Technology Company.

siRNA and plasmid design and transfection

The cell density at the time of transfection should reach 50%–60%. Dilute siRNA and X-treme Gene siRNA Transfection Reagent (Roche Applied Science, Mannheim, Germany) with the right amount of DMEM respectively. 5 min later, mix the diluted siRNA and X-treme in equal volume. 15 min later, add the volume of the mixture to 2 mL per 5×10^5 cells. After 4–6 h of incubation in the cell incubator, switch to 5% DMEM, and continue to culture for 24 h for further processing. The specific siRNA targeted at knocking down RPS6 was synthesized by Ribobio (Guangzhou, China). The sequences were as follows, si-RPS6, 5′-AGGCCTTTACTAAGATTAA-3′.

Immunofluorescence

The cultured cells or tissue sections were fixed with 4% paraformaldehyde at room temperature for 30 min and then washed 3 times with PBS. 0.3% Triton X-100 was added for 30 min at 37°C. 5% BSA was added for 30 min, followed by incubation with anti-Ki67 antibody (1:100), anti-RPS4XL antibody (1:50), or anti-Flag (1:1,000) in PBS at 4°C overnight. After three washes with PBS, cells were incubated with fluorescently labeled secondary antibody (1:50) diluted with PBS at 37°C for 2 h. Finally, DAPI (1:10) was incubated at room temperature for 15 min. Images were acquired by confocal laser scanning microscope (CLSM).

Immunohistochemistry

After the paraffin sections were dewaxed, they were soaked in the configured heated sodium citrate solution and placed in a microwave oven for 15 min on high heat. After completion of antigen retrieval, they were cooled at room temperature. Samples were then blocked with 3% H_2O_2 in PBS at room temperature and subjected to antigen retrieval. Next, sections were incubated with primary antibodies RPS4XL (1:500) at 4°C overnight, incubated with biotinylated secondary antibodies, and subjected to diaminobenzidine staining. Images were acquired by CLSM.[53]

Western blot analysis

Separation of denatured proteins from mice lung tissues or PASMCs with 8%–12% polyacrylamide gels was performed. The protein was transferred from the gel to the nitrocellulose membrane. Primary antibodies against cyclin A (1:250), cyclin D1 (1:200), cyclin E (1:500), CDK1 (1:400), CDK2 (1:500), proliferating cell nuclear antigen (PCNA; 1:200), RPS6 (1:500), p-RPS6 (1:500) Flag (1:1,000), and RPS4XL (1:2,000) were used, with β-actin (1:4,000) as an internal control.

Scratch-wound assay

PASMCs cultured in 6-well plates. When cells grew to 95%, cells were transfected. After transfection, cells were wounded with pipette tips, and the ablated cells were removed by washing with PBS. The cells were then divided into normoxic and hypoxic groups. Wounded areas were photographed immediately (0 h) and at 24 h after incubation. And the wound closure area was calculated as follows: migration area (%) = (A0 −An)/A0 × 100, where A0 represents the area of the original wound area.

Purification and use of exogenous peptides

The latest codon optimization software MaxCodon Optimization Program (V13) developed by Detai Bio (Nanjing, China) was used to optimize the aa sequence of the RPS4XL protein. The whole gene synthesis was used and the Rps4l gene was inserted into the expression vector pET30a through the restriction enzyme sites NdeI and HindIII. The accuracy of the final expression vector by enzyme digestion and sequencing was confirmed and finally transferred to Top10 clone strain and BL21(DE3) expression strain, respectively, and expression of Rps4l protein was induced by IPTG (Isopropyl-β-D-thiogalactoside), and then the RPS4XL protein was purified by affinity chromatography (Ni-IDA resin). The purified protein was added to mouse PASMCs and human PASMCs at concentrations of 5 μg/mL, 7.5 μg/mL, and 10 μg/mL.

Construction of serotype 9 AAV9 and the hypoxic animal model

The corresponding target RNA cloning construction and virus packaging experiment were successfully completed by Shanghai Genechem (Shanghai, China). An aliquot of the vector at 10^{10}–10^{11} genome equivalents was prepared in 20–30 μL in HBSS (Hank's

balanced salt solution). Mice weighing approximately 25 g each were randomly divided into different groups, and isoflurane anesthesia was followed by nasal drops. The corresponding normoxia or hypoxia treatment were performed according to the grouping needs as described earlier. After culturing for 21 days, the corresponding indicators were detected, and after anesthesia with isoflurane, lung tissues were taken for corresponding experiments.

Bioinformatics analysis
The coding ability of Rps4l was analyzed using CPC2 (http://cpc2.cbi.pku.edu.cn/) and PhyloCSF (http://genome.ucsc.edu/). The ORF was analyzed by ExPASy (https://www.expasy.org/). The peptide is modeled using SWISS-MODEL (https://swissmodel.expasy.org/). The protein-protein interaction network was analyzed by STRING (https://string-db.org/) and was then visualized using the Cytoscape program (https://cytoscape.org/).

Statistical analysis
Data are expressed as mean ± SEM and were analyzed with SPSS 13.0 software (SPSS, Chicago, IL, USA). Statistical comparisons among multiple groups were performed using analysis of variance (ANOVA) followed by Dunnett's test. Student's t tests were carried out for comparisons between two groups. A two-tailed $p < 0.05$ indicated a statistically significant difference. Non-linear least-square curve fitting of raw data points was performed with GraphPad Prism software (GraphPad Software, San Diego, CA, USA).

SUPPLEMENTAL INFORMATION
Supplemental Information can be found online at https://doi.org/10.1016/j.ymthe.2021.01.005.

AUTHOR CONTRIBUTIONS
Y.L., J.Z., H.S., Y.C., X.Y., W.L., J.Y., L.Z., X.Z., W.X., Y.J., G.W., and W.S. conducted the experiments; Y.L., J.Z., and D.Z. designed the experiments; and Y.L. and D.Z. wrote the paper.

REFERENCES

1. Boucly, A., Morélot-Panzini, C., Garcia, G., Weatherald, J., Jaïs, X., Savale, L., Montani, D., Humbert, M., Similowski, T., Sitbon, O., and Laveneziana, P. (2020). Intensity and quality of exertional dyspnoea in patients with stable pulmonary hypertension. Eur. Respir. J. 55, 1802108.

2. Maron, B.A., and Galiè, N. (2016). Diagnosis, Treatment, and Clinical Management of Pulmonary Arterial Hypertension in the Contemporary Era: A Review. JAMA Cardiol. 1, 1056–1065.

3. Frumkin, L.R. (2012). The pharmacological treatment of pulmonary arterial hypertension. Pharmacol. Rev. 64, 583–620.

4. Deboeck, G., Niset, G., Lamotte, M., Vachiéry, J.L., and Naeije, R. (2004). Exercise testing in pulmonary arterial hypertension and in chronic heart failure. Eur. Respir. J. 23, 747–751.

5. Robalino, B.D., and Moodie, D.S. (1991). Association between primary pulmonary hypertension and portal hypertension: analysis of its pathophysiology and clinical, laboratory and hemodynamic manifestations. J. Am. Coll. Cardiol. 17, 492–498.

6. Humbert, M., and Guignabert, C. (2019). Pathology and pathobiology of pulmonary hypertension: state of the art and research perspectives. Eur. Respir. J. 53, 1801887.

7. Sindi, H.A., and Russomanno, G. (2020). Therapeutic potential of KLF2-induced exosomal microRNAs in pulmonary hypertension. Nat. Commun. 11, 1185.

8. McLaughlin, V.V., Shah, S.J., Souza, R., and Humbert, M. (2015). Management of pulmonary arterial hypertension. J. Am. Coll. Cardiol. 65, 1976–1997.

9. Luo, H., Zhu, G., Xu, J., Lai, Q., Yan, B., Guo, Y., Fung, T.K., Zeisig, B.B., Cui, Y., Zha, J., et al. (2019). HOTTIP lncRNA Promotes Hematopoietic Stem Cell Self-Renewal Leading to AML-like Disease in Mice. Cancer Cell 36, 645–659.e8.

10. Hu, Q., and Ye, Y. (2019). Oncogenic lncRNA downregulates cancer cell antigen presentation and intrinsic tumor suppression. Nat. Immunol. 20, 835–851.

11. Zampetaki, A., and Mayr, M. (2017). Long Noncoding RNAs and Angiogenesis: Regulatory Information for Chromatin Remodeling. Circulation 136, 80–82.

12. Shen, S., Li, K., Liu, Y., Liu, X., Liu, B., Ba, Y., and Xing, W. (2020). Silencing lncRNA AGAP2-AS1 Upregulates miR-195-5p to Repress Migration and Invasion of EC Cells via the Decrease of FOSL1 Expression. Mol. Ther. Nucleic Acids 20, 331–344.

13. Lu, Z., Yu, Y., Ding, X., Jin, D., Wang, G., Zhou, Y., Zhu, Y., Na, L., He, Y., and Wang, Q. (2020). LncRNA FLJ33360 accelerates the metastasis in hepatocellular carcinoma by targeting miRNA-140/MMP9 axis. Am. J. Transl. Res. 12, 583–591.

14. Gao, Q., Zhou, R., Meng, Y., Duan, R., Wu, L., Li, R., Deng, F., Lin, C., and Zhao, L. (2020). Long noncoding RNA CMPK2 promotes colorectal cancer progression by activating the FUBP3-c-Myc axis. Oncogene 39, 3926–3938.

15. Ballarino, M., Cipriano, A., Tita, R., Santini, T., Desideri, F., Morlando, M., Colantoni, A., Carrieri, C., Nicoletti, C., Musaro, A., et al. (2018). Deficiency in the nuclear long noncoding RNA Charme causes myogenic defects and heart remodeling in mice. EMBO J. 37, e99697.

16. Zahid, K.R., Raza, U., Chen, J., Raj, U.J., and Gou, D. (2020). Pathobiology of pulmonary artery hypertension: role of long non-coding RNAs. Cardiovasc. Res. 116, 1937–1947.

17. Jin, Q., Zhao, Z., Zhao, Q., Yu, X., Yan, L., Zhang, Y., Luo, Q., and Liu, Z. (2020). Long noncoding RNAs: emerging roles in pulmonary hypertension. Heart Fail. Rev. 25, 795–815.

18. Wang, S., Cao, W., Gao, S., Nie, X., Zheng, X., Xing, Y., Chen, Y., Bao, H., and Zhu, D. (2019). TUG1 Regulates Pulmonary Arterial Smooth Muscle Cell Proliferation in Pulmonary Arterial Hypertension. Can. J. Cardiol. 35, 1534–1545.

19. Xing, Y., Zheng, X., Fu, Y., Qi, J., Li, M., Ma, M., Wang, S., Li, S., and Zhu, D. (2019). Long Noncoding RNA-Maternally Expressed Gene 3 Contributes to Hypoxic Pulmonary Hypertension. Mol. Ther. 27, 2166–2181.

20. Zhang, H., Liu, Y., Yan, L., Wang, S., Zhang, M., Ma, C., Zheng, X., Chen, H., and Zhu, D. (2019). Long noncoding RNA Hoxaas3 contributes to hypoxia-induced pulmonary artery smooth muscle cell proliferation. Cardiovasc. Res. 115, 647–657.

21. Eckhart, L., Lachner, J., Tschachler, E., and Rice, R.H. (2020). TINCR is not a noncoding RNA but encodes a protein component of cornified epidermal keratinocytes. Experimental Dermatology 29, 376–379.

22. Huang, J.Z., Chen, M., Chen, D., Gao, X.C., Zhu, S., Huang, H., Hu, M., Zhu, H., and Yan, G.R. (2017). A Peptide Encoded by a Putative lncRNA HOXB-AS3 Suppresses Colon Cancer Growth. Mol. Cell 68, 171–184.e6.

23. Zhu, S., Wang, J., He, Y., Meng, N., and Yan, G.R. (2018). Peptides/Proteins Encoded by Non-coding RNA: A Novel Resource Bank for Drug Targets and Biomarkers. Front. Pharmacol. 9, 1295.

24. Liu, Y., Zhang, H., Li, Y., Yan, L., Du, W., Wang, S., Zheng, X., Zhang, M., Zhang, J., Qi, J., et al. (2020). Long Noncoding RNA Rps4l Mediates the Proliferation of Hypoxic Pulmonary Artery Smooth Muscle Cells. Hypertension 76, 1124–1133.

25. Wang, Y., Wu, S., Zhu, X., Zhang, L., Deng, J., Li, F., Guo, B., Zhang, S., Wu, R., Zhang, Z., et al. (2020). LncRNA-encoded polypeptide ASRPS inhibits triple-negative breast cancer angiogenesis. J. Exp. Med. 217, 20190950.

26. Spencer, H.L., Sanders, R., Boulberdaa, M., Meloni, M., Cochrane, A., Spiroski, A.M., Mountford, J., Emanueli, C., Caporali, A., Brittan, M., et al. (2020). The LINC00961 transcript and its encoded micropeptide, small regulatory polypeptide of amino acid response, regulate endothelial cell function. Cardiovasc. Res. 116, 1981–1994.

27. Xing, Y., Zheng, X., Fu, Y., Qi, J., Li, M., Ma, M., Wang, S., Li, S., and Zhu, D. (2019). Long Noncoding RNA-Maternally Expressed Gene 3 Contributes to Hypoxic Pulmonary Hypertension. Mol. Ther. 27, 2166–2181.

28. Han, Y., Liu, Y., Yang, C., Gao, C., Guo, X., and Cheng, J. (2020). LncRNA CASC2 inhibits hypoxia-induced pulmonary artery smooth muscle cell proliferation and migration by regulating the miR-222/ING5 axis. Cell. Mol. Biol. Lett. 25, 21.

29. Choi, S.W., Kim, H.W., and Nam, J.W. (2019). The small peptide world in long non-coding RNAs. Brief. Bioinform. 20, 1853–1864.

30. Matsumoto, A., Pasut, A., Matsumoto, M., Yamashita, R., Fung, J., Monteleone, E., Saghatelian, A., Nakayama, K.I., Clohessy, J.G., and Pandolfi, P.P. (2017). mTORC1 and muscle regeneration are regulated by the LINC00961-encoded SPAR polypeptide. Nature 541, 228–232.

31. Bazzini, A.A., Johnstone, T.G., Christiano, R., Mackowiak, S.D., Obermayer, B., Fleming, E.S., Vejnar, C.E., Lee, M.T., Rajewsky, N., Walther, T.C., and Giraldez, A.J. (2014). Identification of small ORFs in vertebrates using ribosome footprinting and evolutionary conservation. EMBO J. 33, 981–993.

32. Andrews, S.J., and Rothnagel, J.A. (2014). Emerging evidence for functional peptides encoded by short open reading frames. Nat. Rev. Genet. 15, 193–204.

33. Jandl, K., Thekkekara Puthenparampil, H., Marsh, L.M., Hoffmann, J., Wilhelm, J., Veith, C., Sinn, K., Klepetko, W., Olschewski, H., Olschewski, A., et al. (2019). Long non-coding RNAs influence the transcriptome in pulmonary arterial hypertension: the role of PAXIP1-AS1. J. Pathol. 247, 357–370.

34. Omura, J., Habbout, K., Shimauchi, T., Wu, W.H., Breuils-Bonnet, S., Tremblay, E., Martineau, S., Nadeau, V., Gagnon, K., Mazoyer, F., et al. (2020). Identification of Long Noncoding RNA H19 as a New Biomarker and Therapeutic Target in Right Ventricular Failure in Pulmonary Arterial Hypertension. Circulation 142, 1464–1484.

35. Ruiz-Orera, J., Messeguer, X., Subirana, J.A., and Alba, M.M. (2014). Long non-coding RNAs as a source of new peptides. eLife 3, e03523.

36. Lu, S., Zhang, J., Lian, X., Sun, L., Meng, K., Chen, Y., Sun, Z., Yin, X., Li, Y., Zhao, J., et al. (2019). A hidden human proteome encoded by 'non-coding' genes. Nucleic Acids Res. 47, 8111–8125.

37. Robledo, S., Idol, R.A., Crimmins, D.L., Ladenson, J.H., Mason, P.J., and Bessler, M. (2008). The role of human ribosomal proteins in the maturation of rRNA and ribosome production. RNA 14, 1918–1929.

38. Enganti, R., Cho, S.K., Toperzer, J.D., Urquidi-Camacho, R.A., Cakir, O.S., Ray, A.P., Abraham, P.E., Hettich, R.L., and von Arnim, A.G. (2018). Phosphorylation of Ribosomal Protein RPS6 Integrates Light Signals and Circadian Clock Signals. Front. Plant Sci. 8, 2210.

39. Williams, A.J., Werner-Fraczek, J., Chang, I.F., and Bailey-Serres, J. (2003). Regulated phosphorylation of 40S ribosomal protein S6 in root tips of maize. Plant Physiol. 132, 2086–2097.

40. Peng, M., Wang, J., Tian, Z., Zhang, D., Jin, H., Liu, C., et al. (2019). Mir6981Autophagy-mediated degradation exhibits promotion of PHLPP1 protein translation. Autophagy 15, 1523–1538.

41. Bourgeois, A., Bonnet, S., Breuils-Bonnet, S., Habbout, K., Paradis, R., Tremblay, E., Lampron, M.C., Orcholski, M.E., Potus, F., Bertero, T., et al. (2019). Inhibition of CHK 1 (Checkpoint Kinase 1) Elicits Therapeutic Effects in Pulmonary Arterial Hypertension. Arterioscler. Thromb. Vasc. Biol. 39, 1667–1681.

42. Jiang, W., Chen, Y., Song, X., Shao, Y., Ning, Z., and Gu, W. (2019). Pim-1 inhibitor SMI-4a suppresses tumor growth in non-small cell lung cancer via PI3K/AKT/mTOR pathway. OncoTargets Ther. 12, 3043–3050.

43. Das, I., Chen, H., Maddalo, G., Tuominen, R., Rebecca, V.W., Herlyn, M., Hansson, J., Davies, M.A., and Egyházi Brage, S. (2020). Inhibiting insulin and mTOR signaling by afatinib and crizotinib combination fosters broad cytotoxic effects in cutaneous malignant melanoma. Cell Death Dis. 11, 882.

44. Leppek, K., Das, R., and Barna, M. (2018). Functional 5′ UTR mRNA structures in eukaryotic translation regulation and how to find them. Nat. Rev. Mol. Cell Biol. 19, 158–174.

45. Derman, E., and Darnell, J.E. (1974). Relationship of chain transcription to poly(A) addition and processing of hnRNA in HeLa cells. Cell 3, 255–264.

46. Bonnet, S., Boucherat, O., Paulin, R., Wu, D., Hindmarch, C.C.T., Archer, S.L., Song, R., Moore, J.B., Provencher, S., Zhang, L., et al. (2020). Clinical value of non-coding RNAs in cardiovascular, pulmonary, and muscle diseases. AJP Cell Physiology 318, C1–c28.

47. Chun, H.J., Bonnet, S., and Chan, S.Y. (2017). Translational Advances in the Field of Pulmonary Hypertension. Translating MicroRNA Biology in Pulmonary Hypertension. It Will Take More Than "miR" Words. Am. J. Respir. Crit. Care Med. 195, 167–178.

48. Hutchinson, J.A., Shanware, N.P., Chang, H., and Tibbetts, R.S. (2011). Regulation of ribosomal protein S6 phosphorylation by casein kinase 1 and protein phosphatase 1. J. Biol. Chem. 286, 8688–8696.

49. Lu, T., Zhu, Z., Wu, J., She, H., Han, R., Xu, H., and Qin, Z.H. (2019). DRAM1 regulates autophagy and cell proliferation via inhibition of the phosphoinositide 3-kinase-Akt-mTOR-ribosomal protein S6 pathway. Cell Commun. Signal. 17, 28.

50. Mazumder, A.G., Patial, V., and Singh, D. (2019). Mycophenolate mofetil contributes to downregulation of the hippocampal interleukin type 2 and 1β mediated PI3K/AKT/mTOR pathway hyperactivation and attenuates neurobehavioral comorbidities in a rat model of temporal lobe epilepsy. Brain Behav. Immun. 75, 84–93.

51. Zhu, D., Medhora, M., Campbell, W.B., Spitzbarth, N., Baker, J.E., and Jacobs, E.R. (2003). Chronic hypoxia activates lung 15-lipoxygenase, which catalyzes production of 15-HETE and enhances constriction in neonatal rabbit pulmonary arteries. Circ. Res. 92, 992–1000.

52. Ma, C., Li, Y., Ma, J., Liu, Y., Li, Q., Niu, S., Shen, Z., Zhang, L., Pan, Z., and Zhu, D. (2011). Key role of 15-lipoxygenase/15-hydroxyeicosatetraenoic acid in pulmonary vascular remodeling and vascular angiogenesis associated with hypoxic pulmonary hypertension. Hypertension 58, 679–688.

53. Zhang, J., Li, Y., Qi, J., Yu, X., Ren, H., Zhao, X., Xin, W., He, S., Zheng, X., Ma, C., et al. (2020). Circ-calm4 Serves as an miR-337-3p Sponge to Regulate Myo10 (Myosin 10) and Promote Pulmonary Artery Smooth Muscle Proliferation. Hypertension 75, 668–679.